Electronic and optical properties of Al_2O_3/SiO_2 thin films grown on Si substrate

2010 J. Phys. D: Appl. Phys. 43 255301

(http://iopscience.iop.org/0022-3727/43/25/255301)

J. Phys. D: Appl. Phys. **43** (2010) 255301 (7pp) doi:10.1088/0022-3727/43/25/255301

Electronic and optical properties of Al_2O_3/SiO_2 thin films grown on Si substrate

Dahlang Tahir[1,2], Hyuk Lan Kwon[1], Hye Chung Shin[1], Suhk Kun Oh[1], Hee Jae Kang[1,5], Sung Heo[3], Jae Gwan Chung[3], Jae Cheol Lee[3] and Sven Tougaard[4]

[1] Department of Physics, Chungbuk National University, Cheongju 361-763, Korea
[2] Department of Physics, Hasanuddin University, Makassar 90245, Indonesia
[3] Analytical Engineering Center, Samsung Advanced Institute of Technology, Suwun 440-600, Korea
[4] Department of Physics and Chemistry, University of Southern Denmark, DK-5230 Odense M, Denmark

E-mail: hjkang@cbu.ac.kr

Received 14 January 2010, in final form 20 May 2010
Published 10 June 2010
Online at stacks.iop.org/JPhysD/43/255301

Abstract
The electronic and optical properties of Al_2O_3/SiO_2 dielectric thin films grown on Si(1 0 0) by the atomic layer deposition method were studied by means of x-ray photoelectron spectroscopy and reflection electron energy loss spectroscopy (REELS). The band gaps of the Al_2O_3/SiO_2 thin films before annealing and after annealing were 6.5 eV and 7.5 eV, respectively, and those of the γ-Al_2O_3 and α-Al_2O_3 phases were 7.1 eV and 8.4 eV, respectively. All of these were estimated from the onset values of the REELS spectra. The dielectric functions were determined by comparing the effective cross-section determined from experimental REELS with a rigorous model calculation based on dielectric response theory, using available software packages. The determined energy loss function obtained from the Al_2O_3/SiO_2 thin films before annealing showed a broad peak at 22.7 eV, which moved to the γ-Al_2O_3 position at 24.3 eV after annealing. The optical properties were determined from the dielectric function. The optical properties of the Al_2O_3/SiO_2 thin films after annealing were in good agreement with those of γ-Al_2O_3. The changes in band gap, electronic and optical properties of the Al_2O_3/SiO_2 thin films after annealing indicated a phase transition from an amorphous phase to the γ-Al_2O_3 phase after annealing.

(Some figures in this article are in colour only in the electronic version)

1. Introduction

Silicon dioxide (SiO_2) has been used as a gate oxide in complementary metal–oxide–semiconductors (CMOSs) because of its stability at the SiO_2/Si interface as well as its good electrical isolation property. Recently, the gate oxide thickness of CMOS devices has been aggressively scaled down to sub-nanometres for the transistor feature size of less than 50 nm, and it reaches the physical limit originating from quantum tunnelling. To avoid quantum tunnelling, a high-κ gate dielectric layer is needed. The high-κ dielectric layer allows for an increased physical thickness, which reduces leakage current and improves device properties. The basic criteria for choosing gate dielectric materials are the barrier heights that will effectively block holes and electrons, the chemical stability in contact with both silicon substrate and gate materials, and a low density of interface electronic states. Among many possible candidates, transition metal oxides such as hafnium dioxide (HfO_2) [1, 2], zirconium dioxide (ZrO_2) [3] and titanium dioxide (TiO_2) [4], rare earth oxides such as lanthanum aluminium oxides (LaAlO) [5, 6] and metal oxides such as alumina (Al_2O_3) and their compounds with SiO_2 are promising candidates for replacing the SiO_2 gate dielectric [7]. Although an Al_2O_3/SiO_2 thin film does not have a high dielectric constant (∼10), it emerged as one of the

[5] Author to whom any correspondence should be addressed.

promising high-κ candidates due to its chemical and thermal stabilities, and high-barrier offset [4, 6]. The electronic and optical properties of alumina are known to be dependent on the structure and on the phase of aluminium oxide [8–10]. In particular, α-Al_2O_3 thin films have received some attention as a gate oxide material because of their high band offset for electrons and holes which reduces leakage currents.

The electronic and optical properties of gate oxide materials influence the device performance to a considerable extent. Both x-ray photoelectron spectroscopy (XPS) and reflection electron energy loss spectroscopy (REELS) are surface sensitive, and hence they are capable of analysing the electronic and optical properties of dielectric thin films because the low energy loss region reflects the structure of the valence and conduction electrons [11]. In fact, REELS has been successfully used to obtain the electronic and optical properties of ultrathin dielectric thin films [1, 3, 5, 7, 12].

In this study, the chemical states were obtained from XPS spectra, and the band gap, the electronic and optical properties of Al_2O_3/SiO_2 thin films, γ-Al_2O_3 thin films and α-Al_2O_3 (sapphire) were obtained from an analysis of REELS spectra. The electronic and optical properties represented by the dielectric function ε, the refractive index n and the extinction coefficient k of the Al_2O_3/SiO_2 thin films clearly show that they undergo a phase transition from an amorphous phase to the γ-Al_2O_3 phase after annealing at 1200 °C. However, the α-Al_2O_3 phase could not be obtained after annealing at these high temperatures.

2. Experiment

Al_2O_3/SiO_2 thin films were grown on p-Si (1 0 0) substrates by the atomic layer deposition (ALD) method. Prior to growing mixed oxide films, the p-type Si substrates were cleaned using the Radio Corporation of America (RCA) method [13], in which wafers are sequentially immersed for several minutes in an NH_4OH–H_2O_2–H_2O mixture (SC-1) and an HCl–H_2O_2–H_2O mixture (SC-2) at elevated temperatures, and then in dilute HF at room temperature. After the Si surface was cleaned, the SiO_2 thin film was thermally grown using H_2O vapour at a temperature of 800 °C [14]. For Al_2O_3, $Al(CH_3)_3$ was used as the precursor and O_3 vapour served as the oxygen source. The film was grown with the substrate at 450 °C in Ar ambient atmosphere, which was supplied as the purge and carrier gas. The physical thickness of the thin films was about 5 nm. The thin films were annealed up to 1200 °C by the rapid thermal annealing method. The composition of the Al_2O_3 thin films as grown and after annealing did not change, which was estimated by a quantitative analysis of the XPS spectra. The REELS spectra of the samples were measured using an ESCALAB210 instrument and recorded at a constant pass energy of 20 eV. The incident and take-off angles from the surface normal were 55° and 0°, respectively. The primary electron energies were 0.5, 1.0, 1.5 and 2.0 keV. The energy resolution, given by the full width at half maximum (FWHM) of the elastic peak of backscattered electrons, was about 0.8 eV, and the REELS spectra were measured up to 100 eV energy loss.

3. Theoretical background for REELS analysis

3.1. Inelastic-scattering cross-sections and energy loss function (ELF)

We investigate the electronic and optical properties of the thin films through a quantitative analysis of the electron energy loss spectra with the Tougaard-Yubero QUEELS-$\varepsilon(\boldsymbol{k}, \omega)$-REELS software package [15]. The model used in this software package takes into account the inelastic scattering of electrons as they travel through the vacuum above the surface, the surface region and the bulk region of the solid and it also takes into account the interference effects between the excitations. Details about this model can be found elsewhere [15–17]. Here we describe the theory briefly. All excitations are described by the dielectric function $\varepsilon(\boldsymbol{k}, \omega)$ of the material, which is the only input into the theoretical calculation. The software calculates the average theoretical electron inelastic scattering cross-section $K_{\mathrm{th}}(E_0, \hbar\omega)$ of all the electrons in a given REELS experiment. Here, E_0 is the primary electron energy and $\hbar\omega$ is the energy lost by the electron in a scattering event. The theoretical inelastic scattering cross-section is compared with an experimental cross-section and in an iterative process this allows us to determine the dielectric function of the thin film. The experimental cross-section $K_{\mathrm{exp}}(\hbar\omega)$ times the corresponding inelastic mean free path λ, in the form of λK_{exp}, is deduced from the measured REELS spectrum by the formula in [18] which is implemented in the QUASES-XS-REELS software. To model the ELF of the materials, we use an expansion involving Drude–Lindhard type oscillators [19, 20] in the form

$$\mathrm{Im}\left[\frac{1}{\varepsilon\,(\boldsymbol{k}, \hbar\omega)}\right] = \sum_{i=1}^{n} \frac{A_i \gamma_i \hbar\omega}{\left((\hbar\omega_{0ik})^2 - \hbar^2\omega^2\right)^2 + \gamma_i^2 \Delta E^2} \cdot \theta\left(\hbar\omega - E_{\mathrm{g}}\right), \tag{1}$$

where

$$\hbar\omega_{0ik} = \hbar\omega_{0i} + \alpha_i \frac{\hbar^2 \boldsymbol{k}^2}{2m}. \tag{2}$$

Here, A_i, γ_i, $\hbar\omega$ and α_i are the strength, damping coefficient, excitation energy and momentum dispersion coefficient of the ith oscillator, respectively, and $\hbar\boldsymbol{k}$ is the transferred momentum of the electron to the solid. Even though the dependence of ω_{0i} on $\boldsymbol{k}$ is generally unknown, we made use of equation (2) with α_i as an adjustable parameter. The values of the momentum dispersion coefficients α_i are related to the effective mass of the electrons. As a general rule, for metals $\alpha_i \sim 1$ for oscillators with $\hbar\omega_i < 30$ eV, and $\alpha_i \sim 0$ for oscillators with $\hbar\omega_i > 30$ eV. However, for semiconductor oxides with high band gaps, $\alpha_i \sim 0$ for all oscillators. The step function $\theta(\hbar\omega - E_{\mathrm{g}})$ is included to describe the effect of the band gap E_{g} in semiconductors and insulators, so that $\theta(\hbar\omega - E_{\mathrm{g}}) = 0$ if $\hbar\omega < E_{\mathrm{g}}$ and $\theta(\hbar\omega - E_{\mathrm{g}}) = 1$ if $\hbar\omega > E_{\mathrm{g}}$. The band gap was estimated from the onset value of energy loss in the REELS spectrum in figure 2. The method was described in our previous work [1, 3, 5, 7].

The oscillator strengths are adjusted to make sure that they fulfil the Kramers–Kronig sum rule [16, 17, 19],

$$\frac{2}{\pi}\int_0^\infty \mathrm{Im}\left\{\frac{1}{\varepsilon\,(\hbar\omega)}\right\}\frac{\mathrm{d}\,(\hbar\omega)}{\hbar\omega} = 1 - \frac{1}{n^2}, \tag{3}$$

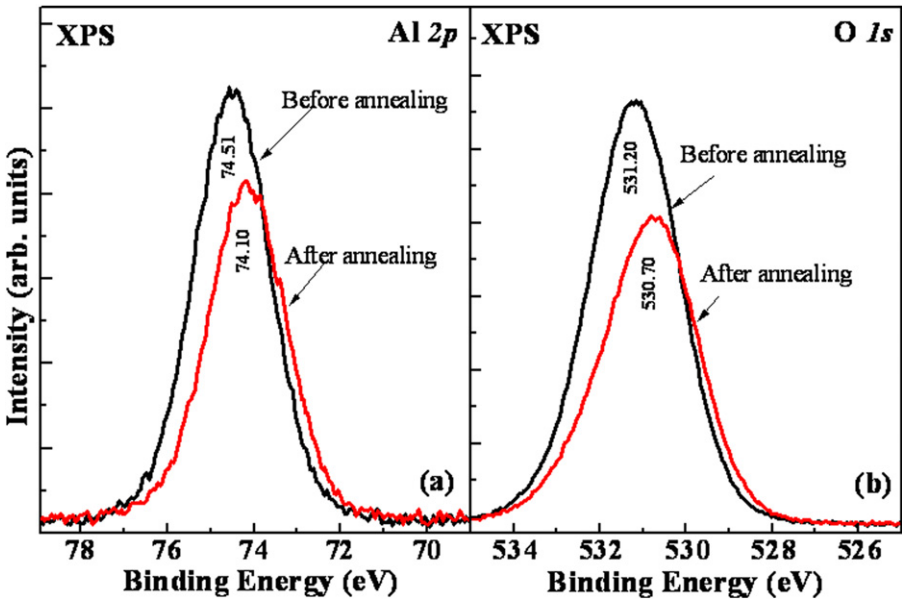

Figure 1. XPS core level photoelectron spectra of (*a*) Al 2p and (*b*) O 1s for Al_2O_3/SiO_2 grown on Si substrate before annealing and after annealing.

where we have used the index of refraction n in the static limit for the optical data. For the Al_2O_3 thin film, it is 1.75 [21]. Actually, the accuracy of this value for the model is not critical in the calculation.

3.2. Optical properties obtained from the ELF

The properties of the electronic states of materials are described by the complex dielectric function of the medium through which the electrons are travelling. The functional shape of the ELF, which is closely related to the features appearing in the experimental loss spectra, led us to parametrize the ELF instead of the dielectric function ε. This parametrization allows us to perform an analytical Kramers–Kronig transformation of $\mathrm{Im}\{1/\varepsilon\}$ to obtain the real part $\mathrm{Re}\{1/\varepsilon\}$ of the reciprocal of the complex dielectric function as follows [19, 20]:

$$\mathrm{Re}\left[\frac{1}{\varepsilon\,(\boldsymbol{k},\hbar\omega)}\right] = 1 - \sum_{i=1}^{n} \frac{A_i\gamma_i\hbar\omega}{\left((\hbar\omega_{0ik})^2 - \hbar\omega\right)^2 + \gamma_i^2\Delta E^2} \cdot\theta\left(\hbar\omega - E_g\right) + \frac{2}{\pi}\int_0^{E_g} \mathrm{Im}\left\{\frac{1}{\varepsilon\,(\boldsymbol{k},z)}\right\}\frac{z\mathrm{d}z}{z^2-\omega^2}. \quad (4)$$

Using $\mathrm{Im}\{1/\varepsilon\}$ and $\mathrm{Re}\{1/\varepsilon\}$, we can express the real and imaginary parts of the dielectric function in the form

$$\varepsilon_1 = \frac{\mathrm{Re}\,\{1/\varepsilon\}}{(\mathrm{Re}\,\{1/\varepsilon\})^2 + (\mathrm{Im}\,\{1/\varepsilon\})^2}, \qquad \varepsilon_2 = \frac{\mathrm{Im}\,\{1/\varepsilon\}}{(\mathrm{Re}\,\{1/\varepsilon\})^2 + (\mathrm{Im}\,\{1/\varepsilon\})^2}. \quad (5)$$

The index of refraction n and the extinction coefficient k are given in terms of the dielectric function as follows [20]:

$$n = \sqrt{\frac{1}{2}\left(\sqrt{\varepsilon_1^2+\varepsilon_2^2}+\varepsilon_1\right)}, \qquad k = \sqrt{\frac{1}{2}\left(\sqrt{\varepsilon_1^2+\varepsilon_2^2}-\varepsilon_1\right)}. \quad (6)$$

Tools to calculate these optical quantities are also included in the QUEELS-$\varepsilon(\boldsymbol{k},\omega)$-REELS software [15].

4. Results and discussion

Figures 1(*a*) and (*b*) show the Al 2p and O 1s photoelectron core level spectra for the Al_2O_3/SiO_2 thin films before annealing and the Al_2O_3/SiO_2 after annealing at 1200 °C, respectively. The measured binding energies of Al 2p and O 1s peaks before annealing are 74.51 eV and 531.20 eV, respectively. The binding energies of Al 2p and O 1s are lowered after annealing. The lowered binding energies of Al 2p (74.10 eV) and O 1s (530.70 eV) peaks suggest a phase transition from an amorphous phase to the γ-Al_2O_3 phase [22, 23].

Figure 2 shows the REELS spectra for the Al_2O_3/SiO_2 on Si substrate thin films (before and after annealing), γ-Al_2O_3, α-Al_2O_3 and SiO_2 thin films at a primary energy of 1.0 keV. The onset of a loss is due to electron–hole excitation and corresponds to the band gap values of the dielectric films. The band gap energy can thus be found by drawing a linear fit line with a maximum negative slope from a point near the onset of the loss spectrum to the background level. The crossing point gives the band gap value [1, 3, 5, 7]. The band gaps of the Al_2O_3/SiO_2 (before annealing), Al_2O_3/SiO_2 (after annealing), γ-Al_2O_3, α-Al_2O_3 and SiO_2 thin films are 6.5 eV, 7.5 eV, 7.1 eV, 8.4 eV and 9.0 eV, respectively. The reproducibility of our fit procedure for the band gap measurements is within ±0.1 eV, which is the standard error of three independent measurements. The band gap of Al_2O_3/SiO_2 changes after annealing to a value close to that of γ-Al_2O_3, and this is attributed to a phase transition from an amorphous phase to the γ-Al_2O_3 phase. Further support for this conclusion is found from the detailed analysis of the ELF and optical properties below.

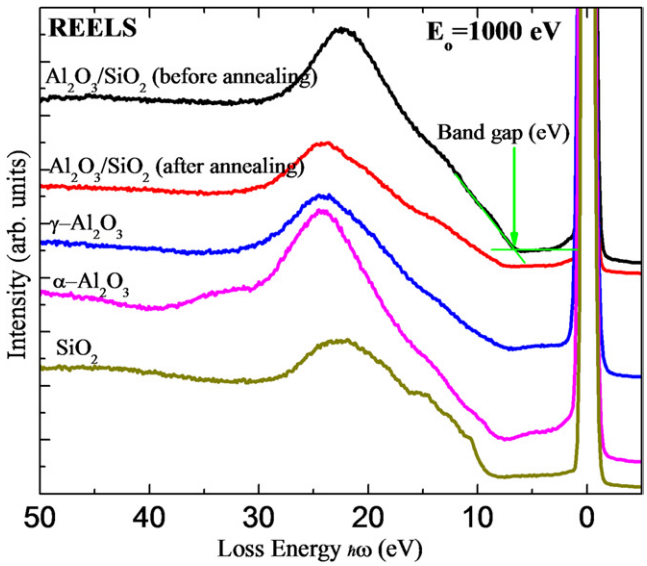

Figure 2. REELS spectra at an energy of 1.0 keV for Al_2O_3/SiO_2 on Si substrate before annealing and after annealing. For comparison, we have also shown the spectra for γ-Al_2O_3, α-Al_2O_3 and SiO_2.

Figure 3 shows good agreement between the experimental inelastic cross-section $\lambda K_{\rm exp}$ (line) and the theoretical inelastic cross-section $\lambda K_{\rm th}$ (symbol) for the Al_2O_3/SiO_2 thin films before and after annealing. We used the QUEELS-XS-REELS software, which is based on the theoretical model in [18], to obtain the experimental $\lambda K_{\rm exp}$ derived from the raw experimental REELS spectra and QUEELS-$\varepsilon(\boldsymbol{k}, \omega)$-REELS software to obtain the theoretical inelastic cross-section $\lambda K_{\rm th}$ at primary electron energies of 1.0, 1.5 and 2.0 keV. The parameters in the ELF were determined by a trial and error procedure, in which the parameters of a test ELF function are adjusted until the agreement between the theoretical inelastic cross-section $K_{\rm th}(E_0, \hbar\omega)$ and the experimental inelastic cross-section $K_{\rm exp}(E_0, \hbar\omega)$ produces a successful fit. The ELF parameters thus determined are shown in table 1. The successful fits in figure 3 using the same ELF for all primary energies give us high confidence in the validity of the model and thereby in the accuracy of the determined ELF. The ELF as well as the surface energy loss function (SELF) for all considered materials corresponding to the determined ELF parameters in table 1 are plotted in figure 4 for a wide energy range (0–80 eV). For comparison, the ELF and SELF spectra of γ-Al_2O_3 and α-Al_2O_3 are also shown in figure 4.

The determined ELF of Al_2O_3/SiO_2 has three oscillators in the vicinity of 14.3, 22.7 and 31 eV before annealing and in the vicinity of 14.3, 24.3 and 31 eV after annealing. These oscillators indicate the loss energy peak position for the electrons travelling in a solid. The probabilities of the ELF for surface and bulk plasmons are given by $\mathrm{Im}[-1/(\varepsilon+1)]$ and $\mathrm{Im}[-1/(\varepsilon)]$ [24], respectively. Both the bulk and surface ELFs of Al_2O_3 before annealing, after annealing, α-Al_2O_3 and γ-Al_2O_3 thin films are shown in figure 4. The main feature in the bulk ELF is a maximum at 24.6 eV for α-Al_2O_3 and at 24.3 eV for γ-Al_2O_3, which is comparable with other results [7]. The energy loss region between 30 and 35 eV is the most pronounced for the α-Al_2O_3; however, it is not the case for either the γ-Al_2O_3 or for the annealed Al_2O_3/SiO_2 thin films. Comparing the parameters in table 1 it is evident that this is due to a much smaller value of the damping coefficient γ and the strength A_i for the oscillator at 31–34 eV for α-Al_2O_3 compared with the other considered materials. The main feature spectrum at 22.7 eV for Al_2O_3/SiO_2 before annealing shifts to a higher energy loss position at 24.3 eV after annealing. The main peak positions of the ELF and SELF after annealing are similar to those of the γ-Al_2O_3 thin films, which are lower than that of α-Al_2O_3. These results suggest a phase transition from an amorphous phase to the γ-Al_2O_3 phase after annealing.

The optical properties for the Al_2O_3/SiO_2, γ-Al_2O_3 and α-Al_2O_3 thin films were determined from the ELF as described in the preceding section as a function of electron energy. Figure 5 shows the real part ε_1 and the imaginary part ε_2 of the dielectric functions. As can be seen in the inset of figure 5(a), the intensity and the main peak of the dielectric function (ε_1 and ε_2) of the Al_2O_3/SiO_2 thin films after annealing are almost identical to those of the γ-Al_2O_3 thin films. The peak of both ε_1 and ε_2 for α-Al_2O_3 is higher than that of the γ-Al_2O_3 thin film. The results in figure 5 show that at the energy where the imaginary part ε_2 has a maximum, the real part ε_1 of the dielectric function decreases to about zero, which indicates a resonance [25]. The resonance in insulators like Al_2O_3 is associated with the collective oscillation of the electrons in the valence band [24]. In metals, the resonance is associated with the collective oscillations of the free electron gas near the Fermi surface, which is excited by the long-range Coulomb interactions. The resonance of free electron gas in metals is much stronger than that of bound electrons in the valence band of insulators [24].

The inset of figure 5(b) shows that the loss energy, for which $\varepsilon_1 \approx \varepsilon_2$, is shifted from 25 eV for the Al_2O_3/SiO_2 thin films before annealing to 26.6 eV after annealing, while the maximum peak position of the ELF changes from 22.7 to 24.3 eV. As expected, the bulk plasmon peak shifts to a higher energy loss position after annealing. In the energy region above the bulk plasmon peak the transparency is higher [20]. Thus, in this energy region, ε_2 (figure 5(b)) and k go to zero as can be clearly seen in figure 6, which shows the values of the refractive index n and the extinction coefficient k as a function of electron energy loss. The intensity and peak position of n of the Al_2O_3/SiO_2 thin films after annealing are almost identical to those of the γ-Al_2O_3 thin films (see the inset of figure 6). Figure 7 shows the reflectivity R of the Al_2O_3/SiO_2, γ-Al_2O_3 thin films and α-Al_2O_3 as a function of electron energy in terms of n and k values as follows [20]:

$$R = \frac{(n-1)^2 + k^2}{(n+1)^2 - k^2}. \tag{7}$$

The reflectivity of Al_2O_3/SiO_2 after annealing for energies <15 eV and >22 eV is practically identical to that of the γ-Al_2O_3 thin films. In the energy loss between 15 and 22 eV, the reflectivity of the γ-$Al_2O_3$is more pronounced than that of Al_2O_3/SiO_2 after annealing. There is a peak at the energy loss

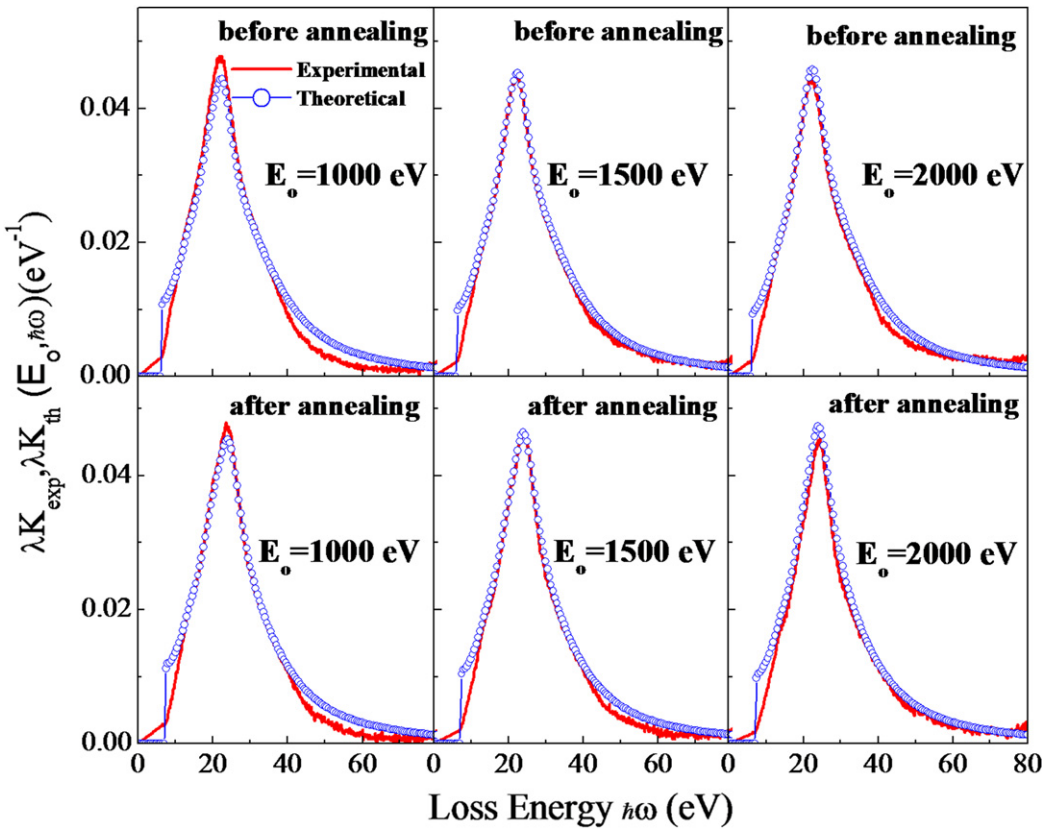

Figure 3. Experimental inelastic cross-section $\lambda K_{\rm exp}$ for Al_2O_3/SiO_2 on Si substrate (line) obtained from REELS data compared with theoretical inelastic cross-sections $\lambda K_{\rm th}$ (symbol) evaluated using the ELF in table 1.

Table 1. Parameters used to model ELFs of Al_2O_3/SiO_2 on Si substrate before annealing, after annealing, γ-Al_2O_3 and α-Al_2O_3 according to the Drude–Lindhard oscillator theory to give the best fit for the experimental cross-section.

	i	$\hbar\omega_{0i}$ (eV)	A_i (eV^2)	γ_i (eV)
Al_2O_3/SiO_2	1	14.3	4.0	6.0
(before annealing)	2	22.7	164.5	7.0
($E_g = 6.5$ eV) ($\alpha_i = 0.02$)	3	31.0	403.0	25.0
Al_2O_3/SiO_2	1	14.3	1.6	4.0
(after annealing)	2	24.3	216.2	7.7
($E_g = 7.5$ eV) ($\alpha_i = 0.02$)	3	31.0	375.4	25.0
γ-Al_2O_3	1	14.5	10.1	6.5
($E_g = 7.1$ eV) ($\alpha_i = 0.02$)	2	24.3	302.8	7.7
	3	34.0	205.6	20.0
α-Al_2O_3	1	14.8	6.0	5.0
($E_g = 8.4$ eV) ($\alpha_i = 0.02$)	2	24.6	325.8	7.7
	3	33.0	177.9	10.0

region between 30 and 35 eV for the α-Al_2O_3, which does not appear for the γ-Al_2O_3 thin films. These reflectivities of both γ-Al_2O_3 and α-Al_2O_3 are similar to those results reported by other groups using vacuum ultraviolet (VUV) and transmission electron energy loss spectroscopy (EELS) [9, 10]. Based on the detailed comparison of n, k, ε_1 and ε_2 above, we conclude that the electronic and optical properties of the Al_2O_3/SiO_2 thin films after annealing are similar to those of the γ-Al_2O_3 thin films.

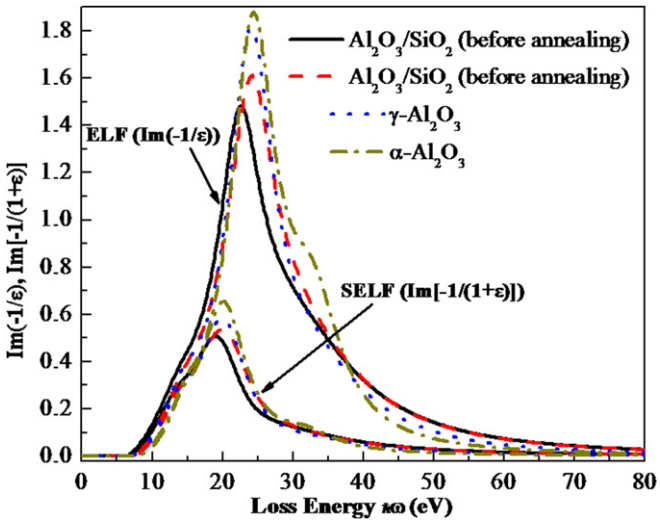

Figure 4. ELFs and SELF of Al_2O_3/SiO_2 on Si substrate before annealing, after annealing, γ-Al_2O_3 and α-Al_2O_3. The ELF parameters are from table 1, which have been used as an input to calculate the $\lambda K_{\rm th}$ values for Al_2O_3/SiO_2 on Si substrate in figure 3.

5. Conclusion

In this work, we obtained the electronic and optical properties of Al_2O_3/SiO_2 and γ-Al_2O_3 thin films and α-Al_2O_3 by means of a quantitative analysis of REELS spectra. The ELFs of the Al_2O_3/SiO_2 and γ-Al_2O_3 thin films and α-Al_2O_3

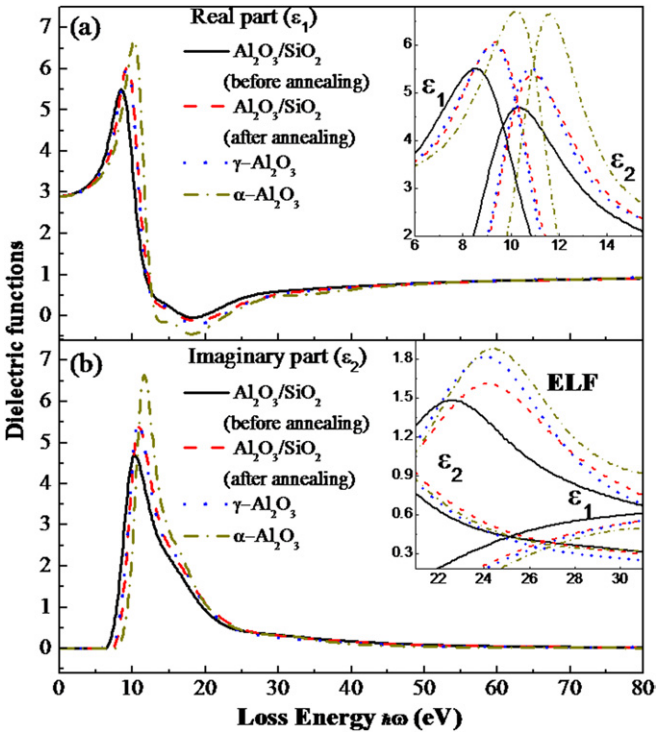

Figure 5. Real part ε_1 and imaginary part ε_2 of the dielectric functions of Al_2O_3/SiO_2 on Si substrate before annealing, after annealing, γ-Al_2O_3 and α-Al_2O_3.

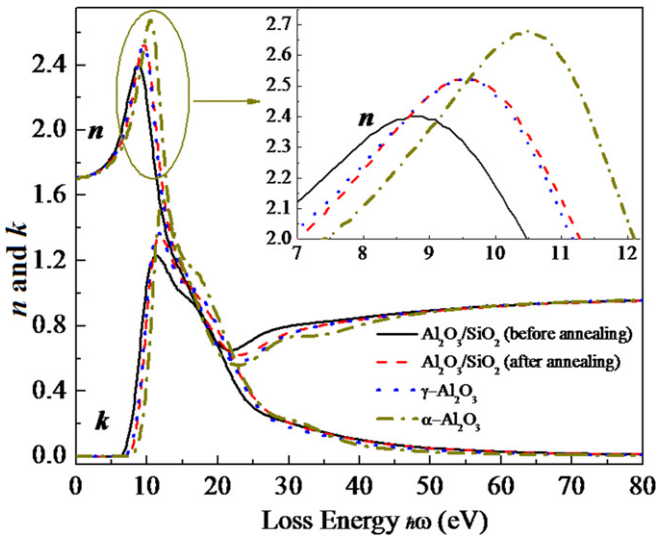

Figure 6. Index of refraction n and extinction coefficient k of Al_2O_3/SiO_2 on Si substrate before annealing, after annealing, γ-Al_2O_3 and α-Al_2O_3.

were obtained by comparing the experimental cross-section $K_{exp}(\hbar\omega)$ times the corresponding inelastic mean free path λ, in the form of λK_{exp}, with the theoretical λK_{th}. The determined ELF of the Al_2O_3/SiO_2 thin film shows a broad peak at 22.7 eV before annealing, which moves to the γ-Al_2O_3 position at 24.3 eV after annealing. The dielectric and optical properties for the Al_2O_3/SiO_2 thin films, γ-Al_2O_3 thin films and α-Al_2O_3 were determined using the ELF. The intensity, the shape and

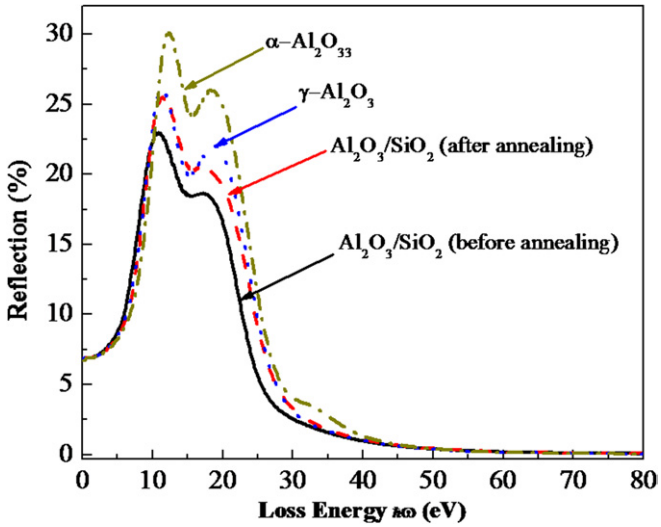

Figure 7. Spectral dependence of the reflectivity R of Al_2O_3/SiO_2 on Si substrate before annealing, after annealing, γ-Al_2O_3 and α-Al_2O_3 determined from the n and k values given in figure 6.

the peak positions of dielectric function (ε_1 and ε_2), and the optical properties (n, k, and R) of the Al_2O_3/SiO_2 thin films after annealing are almost identical to those of the γ-Al_2O_3 thin films but different from those of α-Al_2O_3. It manifested a phase transition from an amorphous phase on the as-grown Al_2O_3/SiO_2 thin films to the γ phase of Al_2O_3 thin films after annealing. The band gap of the Al_2O_3/SiO_2 thin films increased from 6.5 eV to 7.5 eV, and the binding energies of Al 2p and O 1s were lowered by 0.4 eV and 0.5 eV, respectively, after annealing, which was due to this phase transition. The α-Al_2O_3 thin film could not be obtained even after annealing at high temperatures.

Acknowledgment

This work was supported by the Korea Research Foundation Grant funded by the Korean Government (MOEHRD, Basic Research Promotion Fund) (KRF-2008-313-C00225).

References

[1] Jin H, Oh S K, Cho Y J, Kang H J and Tougaard S 2007 *J. Appl. Phys.* **102** 053709
[2] Modreanu M, Parramon J S, Durand O, Servet B, Stchakovsky M, Eypert C, Naudin C, Knowles A, Bridou F and Ravet M F 2006 *Appl. Surf. Sci.* **253** 328
[3] Tahir D, Lee E K, Tham T T, Oh S K, Kang H J, Hua J, Heo S, Park J C, Chung J G and Lee J C 2009 *Appl. Phys. Lett.* **94** 212902
[4] Robertson J 2004 *Eur. Phys. J. Appl. Phys.* **28** 265
[5] Jin H, Cho Y J, Oh S K, Kang H J, Park J C, Heo S and Lee J C 2008 *Appl. Phys. Lett.* **93** 052904
[6] Robertson J 2008 *J. Appl. Phys.* **104** 124111
[7] Jin H, Oh S K, Kang H J and Lee J C 2007 *J. Korean Phys. Soc.* **51** 1042
[8] Snijders P C, Jeurgens L P H and Sloof W G 2002 *Surf. Sci.* **496** 97
[9] Jones D J, French R H, Mullejans H, Loughin S, Dorneich A D and Carcia P F 1999 *J. Mater. Res.* **14** 4337

[10] French R H, Mullejans H and Jones D J 1998 *J. Am. Ceram. Soc.* **81** 2549
[11] Egerton R F 1996 *Electron Energy-Loss Spectroscopy in the Electron Microscopy* 2nd edn (New York: Plenum)
[12] Jin H, Oh S K, Kang H J and Tougaard S 2006 *J. Appl. Phys.* **100** 083713
[13] Keren W 1970 *RCA Rev.* **31** 207
[14] Osaka T and Hattori T 1998 *IEEE Trans. Semicond. Manuf.* **11** 20
[15] Tougaard S and Yubero F 2008 *QUEELS-$\varepsilon(k, \omega)$-REELS: Software Package for Quantitative Analysis of Electron Energy Loss Spectra; Dielectric Function Determined by Reflection Electron Energy Loss Spectroscopy* version 3.0, see http://www.quases.com
[16] Hajati S, Romanyuk O, Zemek J and Tougaard S 2008 *Phys. Rev.* B **77** 245405
[17] Tougaard S and Yubero F 2004 *Surf. Interface Anal.* **36** 824
[18] Tougaard S and Chorkendorff I 1987 *Phys. Rev.* B **35** 6570; information on the QUASES-XS_REELS software can be found at www.quases.com
[19] Yubero F, Fujita D, Ramskov B and Tougaard S 1996 *Phys. Rev.* B **53** 9728
[20] Wooten F 1972 *Optical Properties of Solids* (New York: Academic)
[21] www.luxpop.com
[22] Moulder J F, Stickle W F, Sobol P E and Bomben K D 1995 *Handbook of X-Ray Photoelectron Spectroscopy* ed J Chastain and R C King Jr (Eden Prairie: Physical Electronics, Inc.)
[23] Yoshitake M, Song W, Libra J, Masek K, Sutara F, Matolin V and Prince K C 2008 *J. Appl. Phys.* **103** 033707
[24] Tan G L, DeNoyer L K, French R H, Guittet M J and Soyer M G 2005 *J. Electron Spectrosc. Relat. Phenom.* **142** 97
[25] Bekhti W and Ghamnia M 2004 *Catal. Today* **89** 303